

## Chapter 2

---

# Finite element response sensitivity, probabilistic response and reliability analyses

*Joel P. Conte*

*University of California, San Diego, USA*

*Michele Barbato*

*Louisiana State University, Louisiana, USA*

*Quan Gu*

*AMEC Geomatrix, Newport Beach, USA*

---

**ABSTRACT:** Efficient and accurate analytical tools are needed in earthquake engineering to propagate uncertainties from the seismic input and finite element (FE) model parameters to a probabilistic estimate of the seismic performance through advanced large-scale nonlinear simulations based on the same FE models as those used in deterministic analysis. Sensitivities of the FE response with respect to both model and loading parameters represent an essential ingredient in studying this complex propagation of uncertainties. This chapter presents recent developments in FE response sensitivity analysis based on the Direct Differentiation Method (DDM) for displacement-based, force-based, and three-field mixed finite elements. First-Order Second-Moment (FOSM) approximations of the first- and second-order statistics of the response of structural systems with random/uncertain parameters and subjected to deterministic quasi-static and/or dynamic loads are obtained using DDM-based FE response sensitivities and compared to Monte Carlo simulation results. The probability of a structural response quantity exceeding a specified threshold level is evaluated using the First-Order Reliability Method (FORM) combined with DDM-based FE response sensitivities in the search for the “design point(s)” (DPs). Both time-invariant and time-variant problems are considered. The geometry of limit-state surfaces near the DP(s) is explored in subspaces defined by planes of major principal curvatures. This geometry explains the lack of accuracy of FORM-based solutions in some cases and suggests the development of new improved solution strategies, e.g., the Design Point – Response Surface – Simulation (DP-RS-Sim) method. The examples presented in this study include both structural systems and soil-foundation-structure interaction systems and are based on two types of analysis which are used extensively in earthquake engineering, namely pushover analysis and time history analysis.

## 1 Introduction

Providing a structure with the capability of achieving a target performance over its design life-time is a challenging task for structural engineers. In order to complete this task successfully, the engineer must account correctly during the design process for the existing aleatory and epistemic uncertainties. Thus, proper methods are required for propagating uncertainties from model parameters describing the geometry, the material

## 22 Computational structural dynamics and earthquake engineering

---

behaviours and the applied loadings to structural response quantities used in defining performance limit-states. These methods need also to be integrated with methodologies already well-known to practicing engineers, such as the finite element (FE) method.

This study presents recent developments in response sensitivity, probabilistic response and reliability analyses of structural and geotechnical systems in a general-purpose framework for nonlinear FE response analysis. Current advances are highlighted which cover relevant gaps between response sensitivity computation using the Direct Differentiation Method (DDM) and state-of-the-art FE response-only analysis. This work shows extensions of the DDM which were required for efficient computation of FE response sensitivities of structural and Soil-Foundation-Structure-Interaction (SFSI) systems. Response sensitivity analyses are performed and used in application examples to gain insight into the relative importance of model parameters with regard to system response. Response sensitivities are essential tools in studying the propagation of uncertainties in nonlinear dynamic analysis of structural and SFSI systems.

Examples of probabilistic response analysis using the mean-centred First-Order Second-Moment (FOSM) approximation, time-invariant (First- and Second-Order Reliability Methods, FORM and SORM) and time-variant (mean outcrossing rate computation) reliability analyses are provided to illustrate the methodology presented and its current capabilities and limitations.

A new multidimensional visualization technique is introduced to study the topology of limit-state surfaces near their design point(s) (DPs). A hybrid reliability analysis method, developed using the insight gained from this visualization technique, is introduced and illustrated through an application example.

The response sensitivity, probabilistic response and reliability analysis methods presented are based on nonlinear FE quasi-static pushover and time-history analyses, which are used extensively in earthquake engineering and referred to by structural design codes.

### 2 Finite element response sensitivity analysis

FE response sensitivities represent an essential ingredient for gradient-based optimization methods needed in various subfields of structural engineering such as structural optimization, structural reliability analysis, structural identification, and FE model updating (Ditlevsen & Madsen 1996, Kleiber et al. 1997). Furthermore, FE response sensitivities are extremely useful for gaining deeper insight into the effect and relative importance of system and loading parameters with regard to structural response. The computation of FE response sensitivities to geometric, material and loading parameters requires extension of the FE algorithms for response-only computation. If  $r$  denotes a generic scalar response quantity, the sensitivity of  $r$  with respect to the geometric, material or loading parameter  $\theta$  is defined mathematically as the partial derivative of  $r$  with respect to parameter  $\theta$ , considering both explicit and implicit dependencies, evaluated at  $\theta = \theta_0$ , with  $\theta_0 =$  nominal value taken by the sensitivity parameter  $\theta$  for the FE response analysis.

Response sensitivity computation can be performed using different methods, such as the forward/backward/central Finite Difference Method (FDM) (Kleiber et al. 1997, Conte et al. 2003, 2004), the Adjoint Method (AM) (Kleiber et al. 1997), the Perturbation Method (PM) (Kleiber & Hien 1992), and the Direct Differentiation Method

(DDM) (Kleiber et al. 1997, Conte 2001, Conte et al. 2003, 2004, Gu & Conte 2003, Barbato & Conte 2005, 2006, Zona et al. 2005, 2006, Barbato et al. 2006, 2007, Gu et al. 2007a). The FDM is the simplest method for response sensitivity computation, but is also computationally expensive and can be negatively affected by numerical noise (Haftka & Gurdal 1993, Gu & Conte 2003). The AM is extremely efficient for linear and nonlinear elastic structural systems/models, but is not as efficient computationally as other methods when nonlinear hysteretic material constitutive models are employed (Kleiber et al. 1997). The PM is computationally efficient but generally not very accurate. The DDM, on the other hand, is very general, efficient and accurate and is applicable to any material constitutive model. These advantages can be obtained at the one-time cost of differentiating analytically the space- (finite element) and time- (finite difference) discrete equations governing the structural response and implementing these algorithms for “exact” derivative computation in a FE code.

According to the DDM, the consistent FE response sensitivities are computed at each time step, after convergence is achieved for response computation. Response sensitivity calculation algorithms impact the various hierarchical layers of FE response calculation, namely: (1) the structure level, (2) the element level, (3) the integration point (section for frame/truss elements) level, and (4) the material level. Details on the derivation of the DDM sensitivity equation at the structure level and at the element level for classical displacement-based finite elements, specific software implementation issues, and properties of the DDM in terms of efficiency and accuracy can be found elsewhere (Kleiber et al. 1997, Conte 2001, Conte et al. 2003, Gu & Conte 2003). In this study, some newly developed algorithms and recent extensions are presented which cover relevant gaps between state-of-the-art FE response-only analysis and response sensitivity computation using the DDM.

### **2.1 Response sensitivity algorithm for force-based frame elements**

Recent years have seen great advances in nonlinear analysis of frame structures. These advances were led by the development and implementation of force-based elements (Spacone et al. 1996), which are superior to classical displacement-based elements in tracing material nonlinearities such as those encountered in reinforced concrete beams and columns. In the classical displacement-based frame element, the cubic and linear Hermitian polynomials used to interpolate the transverse and axial displacement fields, respectively, are only approximations of the actual displacement fields in the presence of non-uniform beam cross-section and/or nonlinear material behaviour. On the other hand, force-based frame element formulations stem from equilibrium between section and nodal forces, which can be enforced exactly in the case of a frame element. The exact flexibility matrix can be computed for an arbitrary (geometric) variation of the cross-section and for any section/material constitutive law. Thus, force-based elements enable, at no significant additional computational costs, a drastic reduction in the number of elements required for a given level of accuracy in the simulated response of a FE model of a frame structure.

The established superiority of force-based over classical displacement-based frame elements for response-only computation motivated the extension of the DDM to force-based frame elements. The problem is conceptually more complicated for the

24 Computational structural dynamics and earthquake engineering

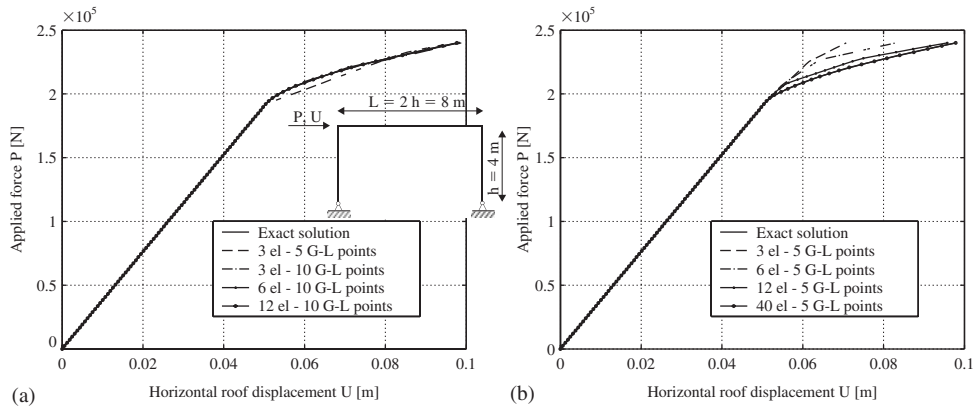


Figure 1 Applied horizontal force versus horizontal roof displacement of different FE meshes: (a) using force-based frame elements and (b) using displacement-based frame elements.

force-based than for the displacement-based element, since in the former no simple direct relation exists between section deformations and the element end deformations. In fact, while equilibrium is enforced in strong form, compatibility is enforced only in weak form over the element. The solution to this problem has been derived and presented elsewhere (Conte et al. 2004). This solution requires solving, at the element level and at each load/time step, a system of linear equations (the size of which depends on the number of integration points for the element) having as unknown the sensitivities of section deformations and element nodal forces. These quantities are necessary for the solution of the sensitivity equation at the structure level. An alternative solution, which does not require solving a system of linear equations at the element level, has been developed and presented in Scott et al. (2004).

The benefit of using force-based instead of displacement-based frame elements has been found even more conspicuous when accurate and efficient computation of structural response sensitivities to material and loading parameters is required in addition to response-only computations (Barbato & Conte 2005). This benefit in terms of improved accuracy and efficiency increases with the complexity of the structural system being analyzed. As application example, a statically indeterminate two-dimensional single-story single-bay steel frame (shown in the inset of Figure 1(a)) with distributed plasticity (modelled by using a Von Mises  $J_2$  plasticity section constitutive law, see Conte et al. 2003) subjected to a horizontal force  $P$  at roof level is presented in this work. Details on the mechanical and geometric properties of the structure and on its modelling can be found in Barbato & Conte (2005). For this simple structure, closed-form solutions are available for horizontal roof displacement and its sensitivities to material parameters as functions of  $P$ . Figures 1(a) and (b) compare the force-displacement results in the horizontal direction obtained from FE analyses employing different meshes of force-based and displacement-based frame elements, respectively. Similarly, Figures 2(a) and (b) compare the sensitivity to the kinematic hardening modulus of the horizontal displacement obtained from FE analyses employing different meshes of force-based and displacement-based frame elements, respectively. It is

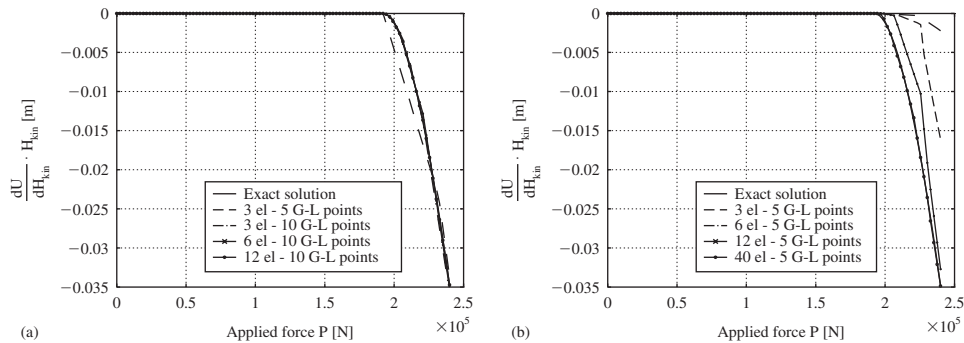


Figure 2 Sensitivities of roof displacement to kinematic hardening modulus for different FE meshes: (a) using force-based frame elements and (b) using displacement-based frame elements.

found that convergence of the FE response to the exact solutions is much faster when force-based elements are employed and this trend is more pronounced for FE response sensitivities.

## 2.2 Response sensitivity algorithm for three-field mixed formulation elements

A large body of research has been devoted to mixed FE formulations in the last 30 years. Several finite elements based on different variational principles have been developed (Washizu 1975, Belytschko et al. 2000) and relationships among them have been established. Accuracy and performance have been thoroughly analyzed and improved and important properties have been recognized and explained, such as equivalence between various stress recovery techniques and ability to eliminate shear-locking effects for specific applications (Belytschko et al. 2000). After more than three decades of research, mixed finite elements are now well established and largely adopted tools in a wide range of structural mechanics applications. Therefore, the advantage of extending the DDM to finite elements based on a mixed formulation is evident.

The DDM algorithm for a three-field mixed formulation based on the Hu-Washizu functional (Washizu 1975) has been derived and presented elsewhere (Barbato et al. 2007). This formulation stems from the differentiation of basic principles (equilibrium, compatibility and material constitutive equations), applies to both material and geometric nonlinearities, is valid for both quasi-static and dynamic FE analysis and considers material, geometric and loading sensitivity parameters. This general formulation has also been specialized to frame elements and linear geometry (small displacements and small strains).

## 2.3 Extension of the DDM to steel-concrete composite frame structures

The last decade has seen a growing interest in FE modelling and analysis of steel-concrete composite structures, with applications to seismic resistant frames and bridges

26 Computational structural dynamics and earthquake engineering

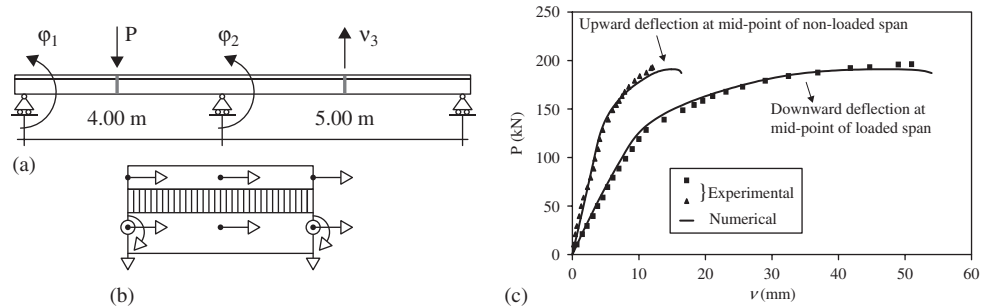


Figure 3 Application example of steel-concrete composite structure: (a) geometry and loading, (b) FE degrees of freedom and (c) comparison of experimental and numerical results.

(Spacone & El-Tawil 2004). The behaviour of composite beams (made of two components connected through shear connectors to form an interacting unit) is significantly influenced by the type of connection between the steel beam and the concrete slab. Flexible shear connectors allow the development of partial composite action. Thus, for accurate analytical response prediction, structural models of composite structures must account for the interlayer slip between the steel and concrete components. A composite beam finite element able to capture the interface slip is therefore an essential tool for model-based response simulation of steel-concrete composite structures.

Compared to common monolithic beams, composite beams with deformable shear connection present additional difficulties. Even in very simple structural systems (e.g., simply supported beams), complex distributions of the interface slip and force can develop. Different finite elements of composite beams with deformable shear connection have been developed and presented in the literature (Spacone & El-Tawil 2004, Dall'Asta & Zona 2004). These elements include suitable models describing section deformations in order to compute the section force resultants of steel-concrete composite members. This requires the use of realistic material constitutive models for beam steel, reinforcement steel, concrete, and shear-slip behaviour of the studs connecting the two structural components (Zona et al. 2005, 2006, Barbato et al. 2007).

The DDM has recently been extended for response sensitivity computation of steel-concrete composite frame structures (Zona et al. 2005, 2006, Barbato et al. 2007). Thus, advanced finite elements incorporating the deformable shear-connection between the two structural components of steel-concrete composite structures can be used for efficient computation of both the response and response sensitivity. Figure 3(a) depicts the configuration and loading condition of a two-span asymmetric continuous steel-concrete composite beam for which experimental data are available. Figure 3(b) shows the degrees of freedom of the frame element (with deformable shear connection) used in modelling this beam structure. Experimental and numerical simulation results are compared in Figure 3(c). It is seen that their agreement is very good.

Figure 4(a) plots the normalized sensitivities (i.e., multiplied by the nominal value of the sensitivity parameter and divided by the current value of the response quantity) of the vertical uplift  $v_3$  at midpoint of the non-loaded span to several material parameters as function of the normalized vertical uplift (i.e., the ratio between the current vertical

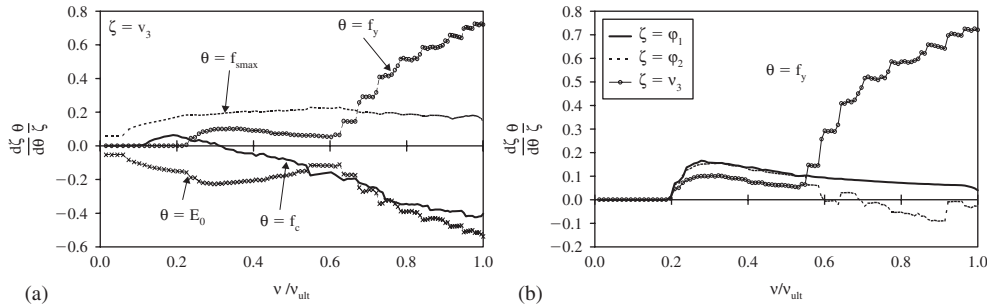


Figure 4 Normalized response sensitivities for steel-concrete composite structure: (a) sensitivities of vertical uplift at midpoint of non-loaded span to several material constitutive parameters and (b) sensitivities of several response quantities to yield strength of the steel of the beam component.

uplift and the maximum uplift which is reached at failure of the beam). The normalized sensitivities can be used directly as importance measures of the sensitivity parameters for the considered response quantity, since they represent the percent change in the response per percent change in the parameter. In the case presented here, the yield strength of the steel of the beam,  $f_y$ , is the parameter affecting the most the vertical uplift  $v_3$ . Figure 4(b) plots the normalized sensitivities of several response quantities to parameter  $f_y$  as functions of the normalized vertical uplift. The effects of parameter  $f_y$  are pronounced for  $v_3$ , but much less so for the rotations of the beam at the left and central supports ( $\varphi_1$  and  $\varphi_2$ , respectively).

#### 2.4 Extension of the DDM to Soil-Foundation-Structure-Interaction (SFSI) systems

The seismic excitation experienced by structures (buildings, bridges, etc.) is a function of the earthquake source (fault rupture mechanism), travel path effects, local site effects, and SFSI effects. Irrespective of the presence of a structure, the local soil conditions (stratification of subsurface materials) may change significantly, through their dynamic filtering effects, the earthquake motion (seismic waves) from the bedrock level to the ground surface. The complex and still poorly understood interactions between subsurface materials, foundations, and the structure during the passage of seismic waves is further significantly complicated by clouds of uncertainties associated with the various components of a SFSI system as well as the seismic excitation.

The DDM has been extended to the analysis of SFSI systems. This extension required development and implementation of response sensitivity algorithms for 2-dimensional (quadrilateral) and 3-dimensional (brick) isoparametric finite elements, soil materials (such as the pressure-independent multi-yield surface plasticity model, see Prevost 1977, Gu et al. 2008b, c) and handling of multipoint constraints (Gu et al. 2008a) required for properly connecting finite elements used in modelling the soil domain with the ones used for the superstructure model (such as frame elements). A benchmark

28 Computational structural dynamics and earthquake engineering

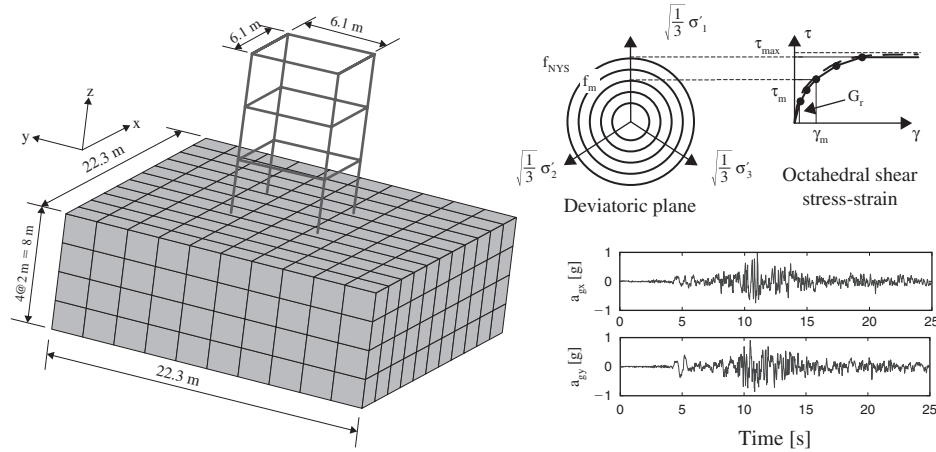


Figure 5 Geometry, input earthquake ground motion and soil material constitutive model for the benchmark SFSI system.

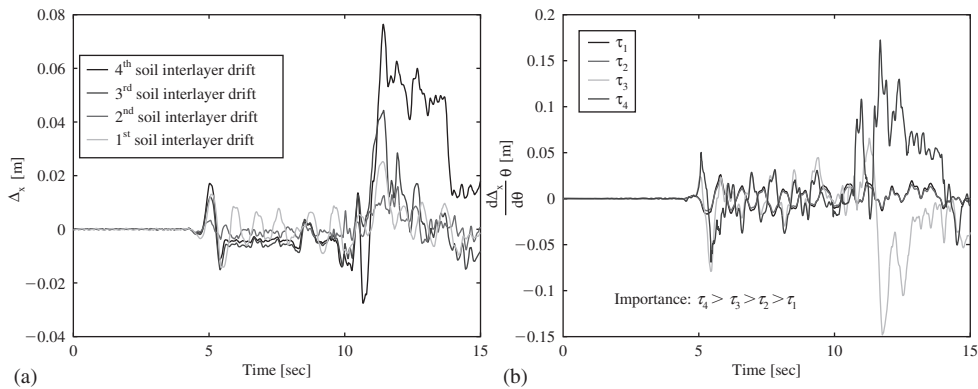


Figure 6 Benchmark SFSI system: (a) time histories of the soil interlayer drifts and (b) sensitivities of the first interstory drift to the shear strengths of the soil layers.

SFSI system is presented in Figure 5. A detailed description of the superstructure can be found in Barbato et al. (2006).

Figure 6(a) plots the time histories of the soil interlayer drifts in the x-direction, while Figure 6(b) shows the first interstory drift in the x-direction,  $\Delta_{1x}$ , sensitivities (multiplied by the nominal value of the sensitivity parameter) to the shear strength parameter of each of the four soil layers. In this case, the parameters affecting the most  $\Delta_{1x}$  are the shear strengths of the two deeper soil layers, since they govern the energy transferred into the structure by the soil from the earthquake input at bedrock level.

## 2.5 Other computational issues in FE response sensitivity analysis

The analytical derivation of FE response sensitivities requires a detailed knowledge of the FE algorithms used for response-only computation, while the efficient computation and reliable use of these sensitivities demand a clear understanding of the analytical properties of the computed response and response sensitivities. These properties for response sensitivities have been investigated in the context of specific applications such as design point search in FE reliability analysis. Some of these properties are discussed below.

A first important issue is the equivalence between two methods for computing FE response sensitivities according to the DDM. Response sensitivities can be computed (1) by differentiating analytically with respect to the sensitivity parameters the time- and space-discrete equations of motion of the structural system considered or (2) by obtaining the time-continuous, space-discrete differential equations governing the response sensitivities and discretizing them in time to numerically compute the response gradient. The conditions of equivalence of these two methods are given in Conte et al. (2003). It is emphasized that consistent (or algorithmic) tangent moduli (leading to consistent tangent stiffness matrices) are to be used in the first method instead of continuum tangent moduli. For uniaxial material constitutive laws, consistent and continuum tangent moduli coincide, which is not the case for multidimensional constitutive models. The consistent tangent moduli have been derived and successfully implemented in FE codes for several multidimensional material constitutive models such as the cap-plasticity model (Conte et al. 2003) (for concrete and geological materials) and the multi-yield-surface plasticity model (Gu et al. 2008b) (for soil).

Continuity/smoothness of FE response sensitivities is another issue needing careful examination, particularly when sensitivities are used in gradient-based optimization algorithms. Gradient discontinuities are detrimental to the rate of convergence or can even impair the convergence to a local minimum of gradient-based optimization algorithms (Gill et al. 1981). It has been recognized that non-smooth material constitutive models exhibit discontinuous response sensitivities corresponding to elastic-to-plastic material state transitions (Conte et al. 2003, Haukaas & Der Kiureghian 2004) while linear elastic unloading events do not produce response sensitivity discontinuities (Haukaas & Der Kiureghian 2004). Recent work established a sufficient condition on the smoothness properties of material constitutive models and loading functions to ensure FE response sensitivity continuity (for both loading and unloading) along the time and parameter axes in the case of quasi-static analysis (Barbato & Conte 2006). The same study also recognized that in the case of dynamic analysis, in addition to smoothness conditions on the material constitutive models employed and the loading functions, a sufficiently fine time-discretization (generally finer than the one required for convergence of response-only computations) is required to avoid response sensitivity discontinuities along the parameter axes.

Finally, the properties of FE response sensitivities have been studied in terms of convergence to the response sensitivities corresponding to the (analytically unknown) solution of the time- and space-continuous equations of motions (Gu & Conte, 2003). The results of these studies indicate that convergence in response sensitivities requires stricter conditions (i.e., finer spatial discretization and, to a lower degree, smaller

load or time step size) than the ones required for convergence of response-only calculations. It is noteworthy that gradient-based optimization algorithms require consistent (and not necessarily converged) gradients in order to preserve the asymptotic rate of superlinear convergence of quasi-Newton methods.

### 3 Simplified finite element probabilistic response analysis

Probabilistic response analysis consists of computing the probabilistic characterization of the response of a specific structure, given as input the probabilistic characterization of material, geometric and loading parameters. An approximate method of probabilistic response analysis is the mean-centred First-Order Second-Moment (FOSM) method, in which mean values (first-order statistical moments), variances and covariances (second-order statistical moments) of the response quantities of interest are estimated by using a mean-centred, first-order Taylor series expansion of the response quantities in terms of the random/uncertain model parameters. Thus, this method requires only the knowledge of the first- and second-order statistical moments of the random parameters. It is noteworthy that often statistical information about the random parameters is limited to first and second moments and therefore probabilistic response analysis methods more advanced than FOSM analysis cannot be fully exploited.

Given the vector of  $n$  random parameters  $\boldsymbol{\theta}$ , the corresponding covariance matrix  $\Sigma_{\boldsymbol{\theta}}$  is defined as

$$\Sigma_{\boldsymbol{\theta}} = [\rho_{ij}\sigma_i\sigma_j]; \quad i, j = 1, 2, \dots, n \quad (1)$$

where  $\rho_{ij}$  = correlation coefficient of random parameters  $\theta_i$  and  $\theta_j$  ( $\rho_{ii} = 1$ ;  $i = 1, 2, \dots, n$ ), and  $\sigma_i$  = standard deviation of random parameter  $\theta_i$ . The vector  $\mathbf{r}$  of  $m$  response quantities of interest is approximated by a first-order truncation of its Taylor series expansion in the random parameters  $\boldsymbol{\theta}$  about their mean values  $\boldsymbol{\mu}_{\boldsymbol{\theta}}$  as

$$\mathbf{r}(\boldsymbol{\theta}) \approx \mathbf{r}_{\text{lin}}(\boldsymbol{\theta}) = \mathbf{r}(\boldsymbol{\mu}_{\boldsymbol{\theta}}) + \nabla_{\boldsymbol{\theta}}\mathbf{r}|_{\boldsymbol{\theta}=\boldsymbol{\mu}_{\boldsymbol{\theta}}} \cdot (\boldsymbol{\theta} - \boldsymbol{\mu}_{\boldsymbol{\theta}}) \quad (2)$$

The first- and second-order statistical moments of the response quantities  $\mathbf{r}$  are approximated by the corresponding moments of the above linearized response quantities, i.e.,

$$\boldsymbol{\mu}_{\mathbf{r}} \approx \boldsymbol{\mu}_{\mathbf{r}_{\text{lin}}} = E[\mathbf{r}_{\text{lin}}(\boldsymbol{\theta})] = \mathbf{r}(\boldsymbol{\mu}_{\boldsymbol{\theta}}) + \nabla_{\boldsymbol{\theta}}\mathbf{r}|_{\boldsymbol{\theta}=\boldsymbol{\mu}_{\boldsymbol{\theta}}} \cdot E[\boldsymbol{\theta} - \boldsymbol{\mu}_{\boldsymbol{\theta}}] = \mathbf{r}(\boldsymbol{\mu}_{\boldsymbol{\theta}}) \quad (3)$$

$$\Sigma_{\mathbf{r}} \approx \Sigma_{\mathbf{r}_{\text{lin}}} = E\left[(\mathbf{r}_{\text{lin}}(\boldsymbol{\theta}) - \boldsymbol{\mu}_{\mathbf{r}_{\text{lin}}}) \cdot (\mathbf{r}_{\text{lin}}(\boldsymbol{\theta}) - \boldsymbol{\mu}_{\mathbf{r}_{\text{lin}}})^T\right] = \nabla_{\boldsymbol{\theta}}\mathbf{r}|_{\boldsymbol{\theta}=\boldsymbol{\mu}_{\boldsymbol{\theta}}} \cdot \Sigma_{\boldsymbol{\theta}} \cdot (\nabla_{\boldsymbol{\theta}}\mathbf{r}|_{\boldsymbol{\theta}=\boldsymbol{\mu}_{\boldsymbol{\theta}}})^T \quad (4)$$

in which  $E[\dots]$  = mathematical expectation operator.

The approximate response statistics computed through Eqs. (3) and (4) are extremely important in evaluating the variability of the response quantities of interest due to the intrinsic uncertainty of the model parameters and provide information on the statistical correlation between the different response quantities. It is noteworthy that these approximate first- and second-order response statistics can be readily obtained when response sensitivities evaluated at the mean values of the random parameters are

FE response sensitivity, probabilistic response and reliability 31

available. Only a single FE analysis is needed in order to perform a FOSM probabilistic response analysis, when the FE response sensitivities are computed using the DDM. Probabilistic response analysis can also be performed using Monte Carlo simulation (MCS). In this study, MCS is used to assess the accuracy of the FOSM approximations in Eqs. (3) and (4) when applied to nonlinear FE response analysis of R/C building structures characterized with random/uncertain material parameters and subjected to quasi-static pushover. The MCS procedure requires:

1. Generation of N realizations of the n-dimensional random parameter vector  $\theta$  according to a given n-dimensional joint probability density function (PDF).
2. Computation by FE analysis of N response curves for each component of the response vector  $r$ , corresponding to the N realizations of the random parameter vector  $\theta$ .
3. Statistical estimation of specified marginal and joint moments of the components of response vector  $r$  at each load step of the FE response analysis.

MCS is a general and robust method for probabilistic response analysis, but it suffers two significant limitations: (1) it requires knowledge of the full joint PDF of random parameters  $\theta$ , which, in general, is only partially known, and (2) it requires performing a usually large number of FE response analyses, which could be computationally prohibitive.

In this study, the Nataf model (Ditlevsen & Madsen 1996) was used to generate realizations of the random parameters  $\theta$ . It requires specification of the marginal PDFs of the random parameters  $\theta$  and their correlation coefficients. It is therefore able to reproduce the given first- and second-order statistical moments of random parameters  $\theta$ . The same three-dimensional three-story reinforced concrete building presented in Section 2.4, but on rigid supports, is considered as application example. Table 1 provides the marginal distributions and their statistical parameters for the material parameters modelled as correlated random variables. Other details on the modelling of the structure and the statistical correlation of the random parameters can be found in Barbato et al. (2006).

Table 1 Marginal PDFs of material parameters (statistical parameters for lognormal distribution: (1)  $\lambda = \mu_{\ln(X)}$ , (2)  $\zeta = \sigma_{\ln(X)}$ ; for beta distribution: (1)  $x_{\min}$ , (2)  $x_{\max}$ , (3)  $\alpha_1$ , (4)  $\alpha_2$ ).

RV	Distribution	Par. #1	Par. #2	Par. #3	Par. #4	Mean	c.o.v. [%]
$f_{c,core}$ [MPa]	Lognormal	3.4412	0.1980	–	–	34.47	20
$\epsilon_{c,core}$ [–]	Lognormal	–5.3973	0.1980	–	–	0.005	20
$f_{cu,core}$ [MPa]	Lognormal	3.0845	0.1980	–	–	24.13	20
$\epsilon_{cu,core}$ [–]	Lognormal	–4.0110	0.1980	–	–	0.02	20
$f_{c,cover}$ [MPa]	Lognormal	3.2180	0.1980	–	–	27.58	20
$\epsilon_{c,cover}$ [–]	Lognormal	–6.3136	0.1980	–	–	0.002	20
$\epsilon_{cu,cover}$ [–]	Lognormal	–5.2150	0.1980	–	–	0.006	20
$f_y$ [MPa]	Beta	227.53	427.48	3.21	4.28	307.46	10.6
$E$ [MPa]	Lognormal	12.1946	0.0330	–	–	201000	3.3
$b$ [–]	Lognormal	–4.0110	0.1980	–	–	0.02	20

## 32 Computational structural dynamics and earthquake engineering

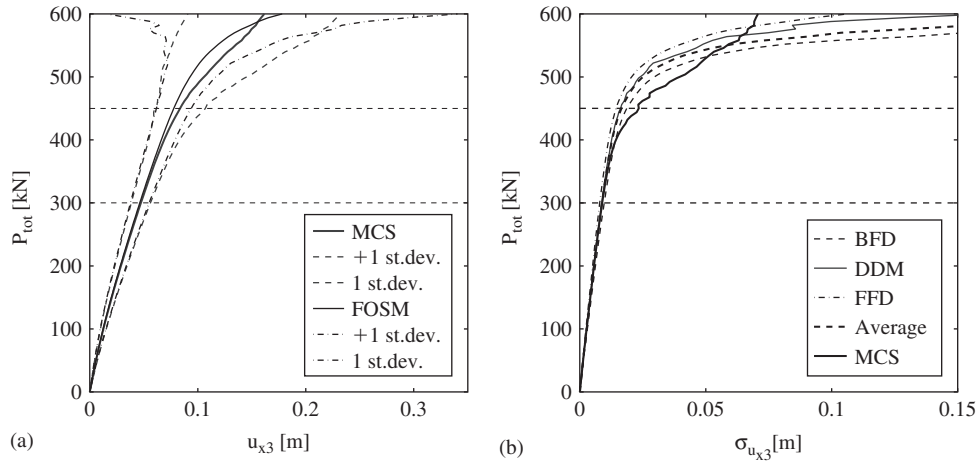


Figure 7 Comparison of probabilistic response analysis results for  $u_{3x}$  obtained from FOSM and MCS: (a) mean value  $\pm$  one standard deviation and (b) standard deviation estimates.

Figure 7(a) compares the estimates of the mean value and mean value  $\pm$  one standard deviation of the roof displacement in the x-direction,  $u_{3x}$ , for a quasi-static pushover analysis with an upper-triangular pattern of applied horizontal forces obtained using FOSM and MCS. Figure 7(b) provides the estimates of the standard deviation of  $u_{3x}$  obtained from MCS and FOSM with sensitivities computed through DDM, backward/forward finite differences (BFD and FFD, respectively, using a small perturbation of each parameter), and the average of BFD and FFD. It is found that a DDM-based FOSM analysis can provide, at low computational cost, estimates of the first- and second-order response statistics which are in good agreement with significantly more expensive MCS estimates when the frame structure experiences low-to-moderate material nonlinearities. Further discussions of these results can be found elsewhere (Barbato et al. 2006).

#### 4 Finite element reliability analysis

In general, the structural reliability problem consists of computing the probability of failure  $P_f$  of a given structure, which is defined as the probability of exceeding some limit-state (or damage-state) function(s) when the loading(s) and/or structural properties and/or limit-state function parameters are uncertain quantities modelled as random variables. This study focuses on component reliability problems, i.e., single limit-state function (LSF)  $g = g(\mathbf{r}, \boldsymbol{\theta})$  where  $\mathbf{r}$  = vector of response quantities of interest and  $\boldsymbol{\theta}$  = vector of random variables considered. The LSF  $g$  is chosen such that  $g \leq 0$  defines the failure domain/region. Thus, the time-invariant component reliability problem can be expressed mathematically as

$$P_f = P[g(\mathbf{r}, \boldsymbol{\theta}) \leq 0] = \int_{g(\mathbf{r}, \boldsymbol{\theta}) \leq 0} p_{\boldsymbol{\theta}}(\boldsymbol{\theta}) d\boldsymbol{\theta} \quad (5)$$

where  $p_{\Theta}(\boldsymbol{\theta})$  = joint PDF of random variables  $\boldsymbol{\theta}$ . For time-variant reliability problems, an upper bound of the probability of failure,  $P_f(T)$ , over the time interval  $[0, T]$ , can be obtained as

$$P_f(T) \leq \int_0^T v_g(t) dt \quad (6)$$

where  $v_g(t)$  = mean down-crossing rate of level zero of the LSF  $g$  and  $t$  = time. An estimate of  $v_g(t)$  can be obtained numerically from the limit form relation (Hagen & Tvedt 1991)

$$v_g(t) = \lim_{\delta t \rightarrow 0} \frac{P[\{g(\mathbf{r}(\boldsymbol{\theta}, t), \boldsymbol{\theta}) > 0\} \cap \{g(\mathbf{r}(\boldsymbol{\theta}, t + \delta t), \boldsymbol{\theta}) \leq 0\}]}{\delta t} \quad (7)$$

Numerical evaluation of the numerator of Eq. (7) reduces to a time-invariant two-component parallel system reliability analysis. It is clear that the first part of Eq. (5) represents the building block for the solution of both time-invariant and time-variant reliability problems (Der Kiureghian 1996). Using Eq. (7), Poisson approximation to the failure probability,  $P_{f,\text{Poisson}}(T)$ , is obtained as (under the hypothesis that  $P[g(\mathbf{r}(\boldsymbol{\theta}, t = 0), \boldsymbol{\theta}) > 0] = 1$ )

$$P_{f,\text{Poisson}}(T) = 1 - \exp\left(-\int_0^T v_g(t) dt\right) \quad (8)$$

The problem posed in Eq. (5) is extremely challenging for real-world structures and can be solved only in approximate ways. A well established methodology consists of introducing a one-to-one mapping/transformation between the physical space of variables  $\boldsymbol{\theta}$  and the standard normal space of variables  $\mathbf{y}$  (Ditlevsen & Madsen 1996) and then computing the probability of failure  $P_f$  as

$$P_f = P[G(\mathbf{y}) \leq 0] = \int_{G(\mathbf{y}) \leq 0} \varphi_Y(\mathbf{y}) d\mathbf{y} \quad (9)$$

where  $\varphi_Y(\mathbf{y})$  = standard normal joint PDF and  $G(\mathbf{y}) = g(\mathbf{r}(\boldsymbol{\theta}(\mathbf{y})), \boldsymbol{\theta}(\mathbf{y}))$  is the LSF in the standard normal space. Solving the integral in Eq. (9) remains a formidable task, but this new form of  $P_f$  is suitable for approximate solutions taking advantage of the rotational symmetry of the standard normal joint PDF and its exponential decay in both the radial and tangential directions. An optimum point at which to approximate the limit-state surface (LSS)  $G(\mathbf{y}) = 0$  is the “design point” (DP), which is defined as the most likely failure point in the standard normal space, i.e., the point on the LSS that is closest to the origin. Finding the DP is a crucial step for approximate methods to evaluate the integral in Eq. (9), such as FORM and SORM and importance sampling

### 34 Computational structural dynamics and earthquake engineering

(IS) (Breitung 1984, Der Kiureghian 1996, Au et al. 1999). The DP,  $\mathbf{y}^*$ , is found as solution of the following constrained optimization problem:

$$\mathbf{y}^* = \arg \{ \min (0.5\mathbf{y}^T\mathbf{y}) | G(\mathbf{y}) = 0 \} \quad (10)$$

The most effective techniques for solving the above constrained optimization problem are gradient-based optimization algorithms (Gill et al. 1981, Liu & Der Kiureghian 1991) coupled with algorithms for accurate and efficient computation of the gradient of the constraint function  $G(\mathbf{y})$ , requiring computation of the sensitivities of response quantities  $\mathbf{r}$  to parameters  $\boldsymbol{\theta}$ . Using the implicit function theorem together with the chain rule of differentiation for multi-variable functions,  $\nabla_{\mathbf{y}}G$  can be obtained as

$$\nabla_{\mathbf{y}}G = (\nabla_{\mathbf{r}}g|_{\boldsymbol{\theta}} \cdot \nabla_{\boldsymbol{\theta}}\mathbf{r} + \nabla_{\boldsymbol{\theta}}g|_{\mathbf{r}}) \cdot \nabla_{\mathbf{y}}\boldsymbol{\theta} \quad (11)$$

where  $\nabla_{\mathbf{r}}g|_{\boldsymbol{\theta}}$  and  $\nabla_{\boldsymbol{\theta}}g|_{\mathbf{r}}$  = gradients of LSF  $g$  with respect to its explicit dependency on quantities  $\mathbf{r}$  and  $\boldsymbol{\theta}$ , respectively, and usually can be computed analytically;  $\nabla_{\boldsymbol{\theta}}\mathbf{r}$  = sensitivities of response variables  $\mathbf{r}$  to parameters  $\boldsymbol{\theta}$ , and  $\nabla_{\mathbf{y}}\boldsymbol{\theta}$  = gradient of physical space parameters with respect to standard normal space parameters. For probability distribution models defined analytically (with monotonically increasing joint CDF), the gradient  $\nabla_{\mathbf{y}}\boldsymbol{\theta}$  can also be derived analytically (Ditlevsen & Madsen 1996).

For real-world problems, the response simulation (computation of  $\mathbf{r}$  for given  $\boldsymbol{\theta}$ ) is typically performed using advanced mechanics-based nonlinear computational models developed based on the FE method. FE reliability analysis requires augmenting existing FE formulations for response-only calculation to compute the response sensitivities,  $\nabla_{\boldsymbol{\theta}}\mathbf{r}$ , to parameters  $\boldsymbol{\theta}$ . As already seen in Section 2, an accurate and efficient way to perform FE response sensitivity analysis is through the DDM.

#### 4.1 Time-invariant reliability analysis

A time-invariant reliability analysis is performed on the same three-story reinforced concrete building as in Sections 2.4 and 3, with the same probabilistic characterization of the material constitutive parameters as well. In addition, the value of the maximum applied horizontal force (equal to the total base shear) is modelled as lognormal random variable (see Figure 8(d)). A roof displacement  $u_{x3} = 0.3$  m (corresponding to a roof drift ratio of 3.1%) is considered as failure condition. First, a DP search is performed (see Figure 8(a)) and a FORM approximation of the probability of failure is obtained. Then, using the DP found in the FORM analysis, a SORM estimate is obtained by computing the first principal curvature at the DP of the LSS and correcting the FORM approximation with Breitung's formula (Breitung 1984). Finally, an IS analysis is performed using as sampling distribution a joint standard normal PDF centred at the DP. It is found that the SORM approximation is distinctly more accurate than the FORM approximation and close to the IS analysis result, which is used here as reference result (Figures 8(b) and (c)).

#### 4.2 Time-variant reliability analysis

The methodology presented in Section 4 for time-variant reliability analysis has been tested on simple structures. Mean up-crossing rates are estimated by FORM (Eq. (7)).

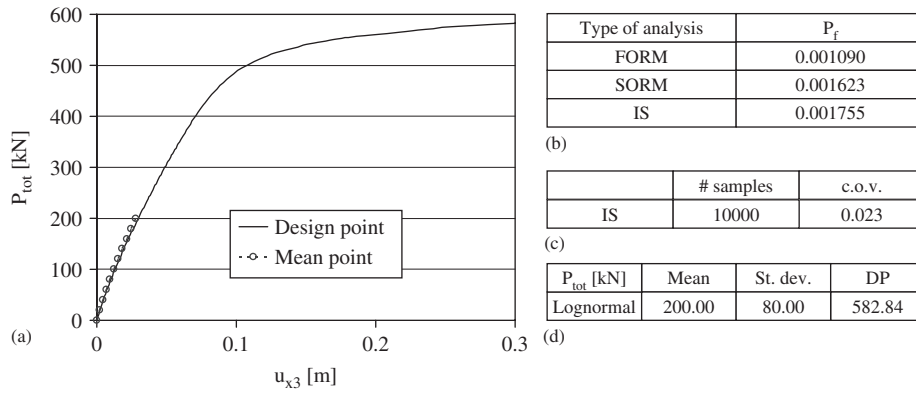


Figure 8 Time-invariant reliability analysis of a 3-story R/C building subjected to pushover loads: (a) Mean and DP pushover curves, (b) comparison of analysis results, (c) IS analysis description, and (d) probabilistic and DP characterization of  $P_{tot}$ .

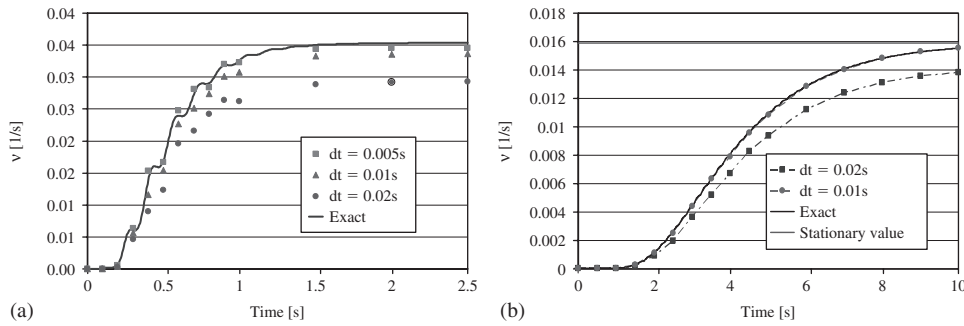


Figure 9 Mean out-crossing computation for linear elastic structures subjected to white noise from at rest initial conditions: (a) SDOF system ( $T = 0.31$  s,  $\zeta = 0.10$ ), and (b) 3-DOF steel building model ( $T_1 = 0.38$  s,  $T_2 = 0.13$  s,  $T_3 = 0.09$  s,  $\zeta_1 = \zeta_3 = 0.02$ , Rayleigh damping).

First, linear elastic SDOF and MDOF structures with at rest initial conditions are subjected to white noise excitation. It is found that the mean up-crossing rates obtained using FORM are in very good agreement with available closed-form solutions (Lutes & Sarkani 1997) as shown in Figures 9(a) and (b) for SDOF and MDOF systems, respectively, when a sufficiently small time-interval,  $dt$ , is used in discretizing the white noise excitation process.

The same methodology is used for SDOF systems with a force-deformation relation modelled using a Menegotto-Pinto (MP) constitutive law (Menegotto & Pinto 1973). This constitutive law is calibrated to a shear-type single-story steel frame with height  $H = 3.20$  m, bay length  $L = 6.00$  m and made of European HE340A steel columns. The system is defined by the following parameters (taken as deterministic): mass  $M = 28800$  kg, damping ratio  $\zeta = 0.02$ , initial stiffness  $K = 40.56$  kN/mm,

36 Computational structural dynamics and earthquake engineering

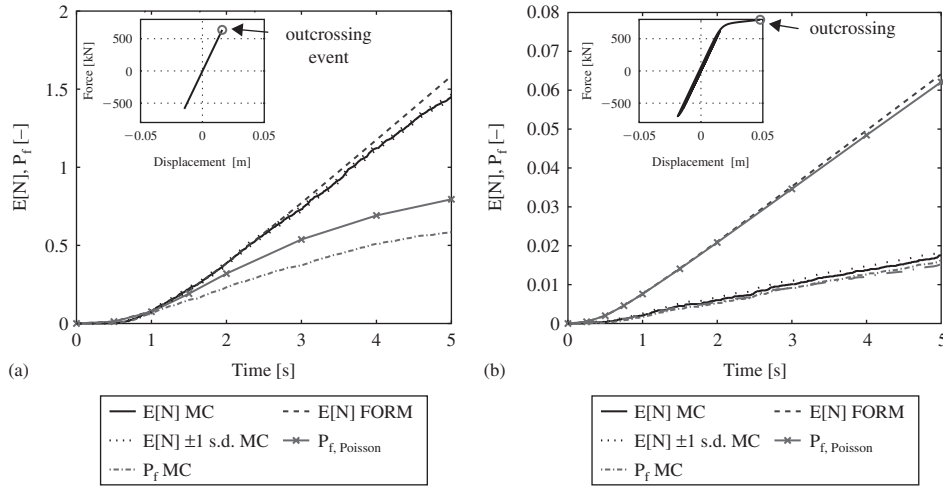


Figure 10 Time-variant reliability analysis results for nonlinear hysteretic SDOF systems: (a) quasi-linear behaviour and (b) significantly nonlinear behaviour.

initial yield force  $F_{y0} = 734$  kN and post-yield to initial stiffness ratio  $b = 0.05$ . This SDOF system is subjected to two different input ground motions modelled as white noises with power spectral density  $\phi_0 = 0.035$   $m^2/s^3$  and  $\phi_0 = 0.25$   $m^2/s^3$ , respectively. The expected cumulative number of up-crossings and time-variant failure probability relative to the roof displacement exceeding the threshold  $\xi = 0.016$  m (roof drift ratio = 0.5%) and  $\xi = 0.048$  m (roof drift ratio = 1.5%), respectively, are computed using FORM and MCS. Figure 10(a) compares the estimates of the expected number of up-crossings obtained using FORM and MCS (with  $\pm$  one standard deviation interval as well) for the case  $\phi_0 = 0.035$   $m^2/s^3$  and  $\xi = 0.016$  m, for which the structure behaves quasi-linearly. Figure 10(a) also compares the time-variant failure probability estimates obtained through the FORM-based Poisson approximation and MCS. Figure 10(b) compares the same estimates as in Figure 10(a), but for the case  $\phi_0 = 0.25$   $m^2/s^3$  and  $\xi = 0.048$  m, for which the structure yields significantly. The insets of Figures 10(a) and (b) provide the DP force-displacement responses for 5.0 s of excitation.

For quasi-linear structural behaviour, the results in terms of expected cumulative number of up-crossings obtained using FORM are in good agreement with the MCS results. In this case, the difference between the FORM-based Poisson approximation and MCS estimate of the time-variant failure probability is mainly due to the relatively high value of  $P_f$ , for which the Poisson assumption of statistically independent up-crossing events is not valid. On the other hand, a FORM approximation of the LSS for significantly nonlinear structural behaviour provides a very inaccurate estimate of the expected cumulative number of up-crossings and therefore of the time-variant failure probability. Thus, computationally efficient methodologies are needed to take into account the nonlinear nature of the LSS for mean out-crossing rate computation.

### 4.3 Limit-state surface topology and multidimensional visualization

Knowledge about the topology (in both the physical and standard normal spaces) of the LSSs corresponding to a given reliability problem is extremely valuable in (1) gaining physical and geometrical insight into the structural reliability problem at hand, (2) analyzing the inaccuracies of the FORM/SORM approximations for time-invariant probability of failure and mean out-crossing rate computation, and (3) pointing to more efficient and accurate computational reliability methods for evaluating the probability content of typical failure domains. The study of the topology of LSSs is a challenging task and requires visualization of nonlinear hyper-surfaces in high-dimensional spaces (i.e., physical or standard normal space defined by random parameters representing loading, geometric and material properties).

A new methodology, herein referred to as Multidimensional Visualization in the Principal Planes (MVPP), is proposed for visualizing the shape of LSSs in FE reliability analysis in the neighbourhood of the DP(s). The MVPP requires finding the trace of the LSS in the planes of principal curvatures at the DP(s) (Principal Planes: PPs) in decreasing order of magnitude of the principal curvatures. Each PP is defined by the DP vector  $\mathbf{y}^*$  and one of the eigenvectors (Principal Direction: PD) of the following Hessian matrix  $\mathbf{A}$  (Der Kiureghian & De Stefano 1991)

$$\mathbf{A} = \frac{\mathbf{H}_{\text{red}}}{\left\| \nabla_{\mathbf{y}} G|_{\mathbf{y}^*} \right\|} \quad (12)$$

in which  $[\mathbf{H}_{\text{red}}]_{i,j} = [\mathbf{R} \cdot \mathbf{H} \cdot \mathbf{R}^T]_{i,j}$  is the reduced Hessian, with  $i, j = 1, 2, \dots, N - 1$  and  $N =$  number of random parameters,  $\mathbf{H} = (N \times N)$  Hessian matrix of the LSF at the DP,  $\mathbf{R} =$  matrix of coordinate transformation so that the new reference system has the  $N$ -th axis oriented as the DP vector  $\mathbf{y}^*$ , and  $\left\| \nabla_{\mathbf{y}} G|_{\mathbf{y}^*} \right\| =$  Euclidean norm of the gradient of the LSF at the DP. The PDs are sorted in decreasing order of magnitude of the corresponding eigenvalues.

In this study, the Hessian matrix is obtained by forward finite difference calculations applied to the DDM-based response sensitivities. For accurate FE models of realistic structural systems with a large number of uncertain model parameters, this approach for computing the Hessian matrix, which is then used to compute the major eigenvalues/eigenvectors, could be computationally prohibitive. Methods are under study for obtaining computationally affordable approximations of the Hessian matrix able to produce sufficiently accurate major eigenvalues/eigenvectors. In addition, the use of an existing algorithm (Der Kiureghian & De Stefano 1991) for computing eigenvalues (and corresponding eigenvectors) in order of decreasing magnitude without having to compute the Hessian matrix is also being considered.

The MVPP methodology provides important information about the topology of the LSS identifying a small number of dimensions which are of interest and thus requiring a limited number of FE simulations to visualize the LSS.

### 4.4 New hybrid method for finite element reliability analysis

As shown in Sections 4.1 and 4.2, FORM approximation of the LSS(s) can provide a very crude estimate of the time-invariant and time-variant (using mean out-crossing

### 38 Computational structural dynamics and earthquake engineering

rate computation) failure probability of a structural system exhibiting a strongly nonlinear material behaviour. Information about the topology of the LSS(s) near the DP(s) can be used effectively in order to improve on the FORM approximation accounting for nonlinearities in the LSF.

A currently under development hybrid time-invariant reliability method, referred to herein as DP-RS-Sim method and able to enhance the FORM/SORM estimates of time-invariant and time-variant failure probabilities for structural and/or geotechnical systems, is briefly presented and illustrated below. The DP-RS-Sim method combines (1) the DP search (used in FORM and SORM), (2) the Response Surface (RS) method to approximate in analytical (polynomial) form the LSF near the DP, and (3) a simulation technique (Sim), to be applied on the response surface representation of the actual LSF.

The proposed method is suitable, with minor variations, for both component and system time-invariant reliability problems and for component mean out-crossing rate computations. The main steps of the DP-RS-Sim method for time-invariant component reliability analysis involving a LSS with a single DP are:

1. Search for the DP (step common to FORM, SORM and the MVPP method).
2. Computation of (few) PDs (step common to SORM with curvature fitting and the MVPP method).
3. Use of RS method to approximate analytically the LSF near the DP as the sum of a nonlinear part (in the few transformed variables defined by the DP vector and the computed PDs) and a linear part (in the remaining transformed variables and defined by the gradient at the DP). This step is unique to the proposed DP-RS-Sim method.
4. Estimate of the time-invariant failure probability using crude MCS or any other more advanced simulation technique (e.g., IS) applied on the analytical response surface approximation of the actual LSF.

In time-invariant system reliability analysis, the DP-RS-Sim method requires repeating the first three steps defined above for each of the components (LSFs) and applying the fourth step after forming a Boolean indicator which provides correspondence between failures of the single components and failure of the system. Time-invariant component reliability analysis with a LSS characterized by multiple DPs can be interpreted as a special case of a time-invariant system reliability problem, with the failure domain given by the union of the failure domains defined by the response surfaces approximating the original LSF in the neighbourhood of each of the DPs. Time-variant component reliability analysis is treated using the DP-RS-Sim method to compute the mean out-crossing rate with the limit relation in Eq. (7), in which the two LSSs  $\{g(\mathbf{r}(\boldsymbol{\theta}, t), \boldsymbol{\theta}) = 0\}$  and  $\{g(\mathbf{r}(\boldsymbol{\theta}, t + \delta t), \boldsymbol{\theta}) = 0\}$  are approximated at their DPs with the RS method.

The use of the DP-RS-Sim method in the case of a time-variant reliability problem is illustrated using the same MP SDOF system defined in Section 4.2 (with deterministic parameters) when subjected to white noise base excitation with power spectral density  $\phi_0 = 0.25 \text{ m}^2/\text{s}^3$  and displacement threshold  $\xi = 0.048 \text{ m}$  (corresponding to the significantly nonlinear behaviour case in Section 4.2). Figures 11(a) and (b) provide visualization of the LSSs at times  $t = 1.0 \text{ s}$  and  $t + \delta t = 1.001 \text{ s}$  using the MVPP method in the first and second PPs, respectively. The traces of these two LSSs (obtained as the

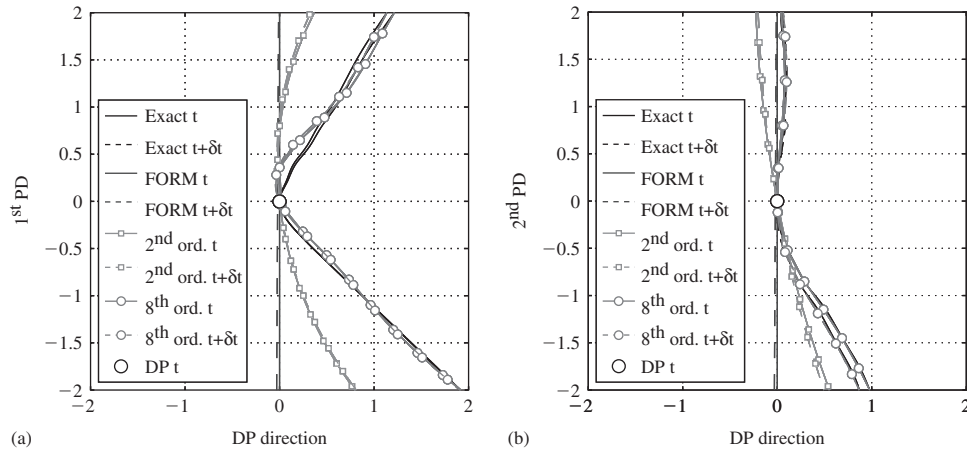


Figure 11 Visualization of LSS by the MVPP method and different response surface approximations for mean up-crossing rate computation at time  $t = 1.0$  s for nonlinear hysteretic MP SDOF system: (a) 1st PP and (b) 2nd PP.

zero level contour lines of the LSF simulated over a fine grid of points in each PP) are compared with different response surface approximations, namely a 1st order (FORM), 2nd order and 8th order polynomial approximation. It is seen that the 8th order response surface approximates the actual LSSs fairly well in the first PP (Figure 11(a)) and very well in the second PP (Figure 11(b)).

The DP-RS-Sim method is applied to compute the time-variant failure probability (for  $T = 5.0$  s) of the inelastic SDOF system defined above. The probability of failure is estimated by integrating numerically the mean out-crossing rate computed at given instants of time ( $t = 0.25$  s,  $0.5$  s,  $0.75$  s,  $1.0$  s,  $1.5$  s,  $2.0$  s,  $3.0$  s,  $4.0$  s and  $5.0$  s). The Gaussian white noise excitation is discretized with  $dt = 0.01$  s into 25, 50, 75, 100, 150, 200, 300, 400, and 500 random variables for these instants of time. Each of the LSFs is approximated with a response surface obtained as the sum of an 8th order polynomial in the four transformed variables defined by the DP vector and the first three principal directions and a 1st order polynomial in the remaining variables (i.e., hyperplane tangent to the LSS at the DP). The probability content of the hyper-wedge defined by the intersection of the two component failure domains, see Eq. (7), is estimated via IS with sampling distribution centred at the DP. Figure 12 compares the results obtained through crude MCS for the expected cumulative number of up-crossings,  $E[N]$ , and the failure probability,  $P_f$ , with the upper bound approximation of the failure probability obtained through FORM and DP-RS-Sim. The results obtained show that the error due to the use of the analytical upper-bound to the probability of failure  $P_f$  is small, while the error due to the use of a FORM approximation to  $E[N]$  is very high (error = 266% at time  $t = 5.0$  s). The DP-RS-Sim method reduces significantly the error by FORM, providing very good estimates of  $E[N]$  (error = 16% at time  $t = 5.0$  s) with a reasonable additional computational cost compared to FORM.

40 Computational structural dynamics and earthquake engineering

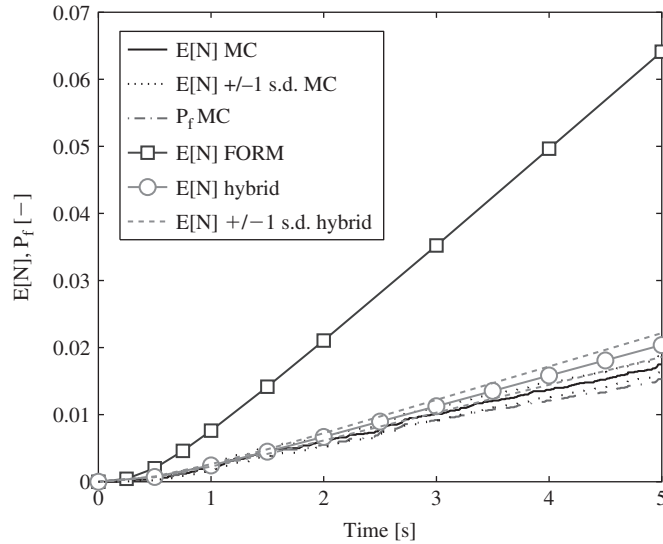


Figure 12 Time-variant reliability analysis of nonlinear hysteretic MP SDOF system: comparison of FORM and DP-RS-Sim (hybrid) method results with Monte Carlo (MC) simulation results.

### 5 Conclusions

This study presents recent advances in finite element (FE) response sensitivity, simplified probabilistic response and reliability analyses of structural and/or geotechnical systems. These developments are integrated into general-purpose frameworks for nonlinear FE response analysis. The objective is to extend the analytical tools used extensively by practicing engineers in order to propagate uncertainties through nonlinear static and dynamic analyses of actual structural and/or geotechnical systems to obtain probabilistic estimates of their predicted performance. Extensions of the Direct Differentiation Method (DDM) to nonlinear material FE models of structural and/or geotechnical systems are presented.

The mean-centred First-Order Second-Moment (FOSM) method is presented as simplified FE probabilistic response analysis method. The FOSM method is applied to probabilistic nonlinear pushover analysis of a structural system. It is found that a DDM-based FOSM analysis can provide, at low computational cost, estimates of first- and second-order FE response statistics which are in good agreement with significantly more expensive Monte Carlo simulation estimates when the frame structure considered in this study experiences low-to-moderate material nonlinearities.

Time-invariant and time-variant reliability analysis capabilities are also illustrated. The geometry of limit-state surfaces near the design point(s) (DPs) is explored in reduced-dimension spaces defined by planes of major principal curvatures at the DP, following a newly developed technique called Multidimensional Visualization in the Principal Planes. This new geometrical insight explains the lack of accuracy of FORM-based solutions in some cases and suggests the use of existing and development

of new improved solution strategies. In particular, a new hybrid reliability method referred to as the DP-RS-Sim method is presented and illustrated through an example of mean out-crossing rate computation for a nonlinear hysteretic single-degree-of-freedom system. The methodology presented in this work allows, in general, obtaining at reasonable computational cost FE reliability analysis results that are sufficiently accurate for engineering purposes.

Extension of the DP-RS-Sim method to nonlinear hysteretic multi-degree-of-freedom FE models of actual structural and/or geotechnical systems is currently under study by the authors.

### Acknowledgements

Supports of this research by the Pacific Earthquake Engineering Research (PEER) Center through the Earthquake Engineering Research Centers Program of the National Science Foundation under Award No. EEC-9701568, the National Science Foundation under Grant No. CMS-0010112, and the main Italian Electricity Company (ENEL) are gratefully acknowledged. Any opinions, findings, conclusions, or recommendations expressed in this publication are those of the authors and do not necessarily reflect the views of the sponsors.

### References

- Au, S.K., Papadimitriou, C. & Beck, J.L. 1999. Reliability of uncertain dynamical systems with multiple design points. *Structural Safety*, 21(2), 113–133.
- Barbato, M. & Conte, J.P. 2005. Finite element response sensitivity analysis: a comparison between force-based and displacement-based frame element models. *Computer Methods in Applied Mechanics and Engineering*, 194(12–16), 1479–1512.
- Barbato, M. & Conte, J.P., 2006. Finite element structural response sensitivity and reliability analyses using smooth versus non-smooth material constitutive models. *International Journal of Reliability and Safety*, 1(1–2), 3–39.
- Barbato, M., Gu, Q. & Conte, J.P. 2006. Response sensitivity and probabilistic response analyses of reinforced concrete frame structures. *Proceedings of the 8th NCEE, San Francisco, April 18–22*.
- Barbato, M., Zona, A. & Conte, J.P. 2007. Finite element response sensitivity analysis using three-field mixed formulation: general theory and application to frame structures. *International Journal for Numerical Methods in Engineering*, 69(1), 114–161.
- Belytschko, T., Liu, W.K. & Moran, B. 2000. *Nonlinear Finite Elements for Continua and Structures*. New York: Wiley.
- Breitung, K. 1984. Asymptotic approximations for multinormal integrals. *Journal of the Engineering Mechanics Division (ASCE)*, 110(3), 357–366.
- Conte, J.P. 2001. Finite element response sensitivity analysis in earthquake engineering. In Spencer & Hu (eds), *Earthquake Engineering Frontiers in the New Millennium*, 395–401.
- Conte, J.P., Vijalapura, P.K. & Meghella, M. 2003. Consistent finite-element response sensitivity analysis. *Journal of Engineering Mechanics (ASCE)*, 129, 1380–1393.
- Conte, J.P., Barbato, M. & Spacone, E. 2004. Finite element response sensitivity analysis using force-based frame models. *International Journal for Numerical Methods in Engineering*, 59, 1781–1820.
- Dall'Asta, A. & Zona, A. 2004. Comparison and validation of displacement and mixed elements for the non-linear analysis of continuous composite beams. *Computers and Structures*, 82 (23–26), 2117–2130.

## 42 Computational structural dynamics and earthquake engineering

- Der Kiureghian, A. & De Stefano, M. 1991. Efficient algorithms for second-order reliability analysis. *Journal of Engineering Mechanics* (ASCE), 117(12), 2904–2923.
- Der Kiureghian, A. 1996. Structural reliability methods in seismic safety assessment: a review. *Journal of Engineering Structures*, 18(6), 412–424.
- Ditlevsen, O. & Madsen, H.O. 1996. *Structural Reliability Methods*. New York: Wiley.
- Gill, P.E., Murray, W. & Wright, M.H. 1981. *Practical Optimization*. London: Academic Press.
- Gu, Q. & Conte, J.P. 2003. Convergence studies in non-linear finite element response sensitivity analysis. *Applications of Statistics and Probability in Civil Engineering, Proceedings of ICASP9, San Francisco, July 6–9*.
- Gu, Q., Barbato, M. & Conte, J.P. 2008a. Handling of constraints in finite element response sensitivity analysis. *Journal of Engineering Mechanics*, (ASCE). Submitted for review.
- Gu, Q., Conte, J.P., Yang, Z. & Elgamal, A. 2008b. Consistent tangent moduli for multi-yield-surface  $J_2$  plasticity material model. *International Journal for Numerical Methods in Engineering*. Submitted for review.
- Gu, Q., Conte, J.P., Yang, Z. & Elgamal, A. 2008c. Finite element response sensitivity analysis of multi-yield-surface  $J_2$  plasticity model by direct differentiation method. *Computer Methods in Applied Mechanics and Engineering*. Submitted for review.
- Haftka, R.T. & Gurdal, Z. 1993. *Elements of Structural Optimization*. Dordrecht: Kluwer Academic Publishers.
- Hagen, O. & Tvedt, L. 1991. Vector process out-crossing as parallel system sensitivity measure. *Journal of Engineering Mechanics* (ASCE), 117(10), 2201–2220.
- Haukaas, T. & Der Kiureghian, A. 2004. Finite element reliability and sensitivity methods for performance-based engineering. *Report PEER 2003/14*, Pacific Earthquake Engineering Research Center, University of California, Berkeley.
- Kleiber, M. & Hien, T.D. 1992. *The Stochastic Finite Element Method. Basic Perturbation Technique and Computer Implementation*. New York: Wiley.
- Kleiber, M., Antunez, H., Hien, T.D. & Kowalczyk, P. 1997. *Parameter Sensitivity in Nonlinear Mechanics: Theory and Finite Element Computation*. New York: Wiley.
- Liu, P.-L. & Der Kiureghian, A. 1991. Optimization algorithms for structural reliability. *Structural Safety*, 9(3), 161–177.
- Lutes, L.D. & Sarkani, S. 1997. *Stochastic Analysis of Structural and Mechanical Vibrations*. Upper Saddle River: Prentice Hall.
- Menegotto, M. & Pinto, P.E. 1973. Method for analysis of cyclically loaded reinforced concrete plane frames including changes in geometry and non-elastic behavior of elements under combined normal force and bending. *Proceedings, IABSE Symposium*, Lisbon.
- Prevost, J.H. 1977. Mathematical modelling of monotonic and cyclic undrained clay behaviour. *International Journal for Numerical and Analytical Methods in Geomechanics*, 1(2), 195–216.
- Spacone, E., Filippou, F.C. & Taucer, F.F. 1996. Fibre beam-column element for nonlinear analysis of R/C frames. Part I: formulation. *Earthquake Engineering and Structural Dynamics*, 25(7), 711–725.
- Spacone, E. & El-Tawil, S. 2004. Nonlinear analysis of steel-concrete composite structures: state-of-the-art. *Journal of Structural Engineering*, 130(2), 159–168.
- Scott, M.H., Franchin, P., Fenves, G.L. & Filippou, F.C. 2004. Response sensitivity for nonlinear beam-column elements. *Journal of Structural Engineering* (ASCE), 130(9), 1281–1288.
- Washizu, K. 1975. *Variational methods in elasticity and plasticity*. Oxford: Pergamon Press.
- Zona, A., Barbato, M. & Conte, J.P. 2005. Finite element response sensitivity analysis of steel-concrete composite beams with deformable shear connection. *Journal of Engineering Mechanics* (ASCE), 131(11):1126–1139.
- Zona, A., Barbato, M. & Conte, J.P. 2006. Finite element response sensitivity analysis of continuous steel-concrete composite girders, *Steel and Composite Structures, an International Journal*, 6(3), 183–202.